*Clays and Clay Minerals*, Vol. 34, No. 3, 295–306, 1986.

# ISOTHERMAL DIFFUSION OF Eu AND Th IN DEEP-SEA SEDIMENTS: EXPERIMENTAL RESULTS AND A NUMERICAL MODEL

GERALD B. EPSTEIN

Graduate School of Oceanography, University of Rhode Island
Kingston, Rhode Island 02882

G. ROSS HEATH

College of Ocean and Fishery Sciences HA-40, University of Washington
Seattle, Washington 98195

**Abstract**—Batch data for the sorption of Eu and Th on pelagic sediments may be represented by equations of the form: $\ln M = A \ln C_s + B/T + D$, where M = concentration of sorbate on sediment, $C_s$ = concentration of sorbate in solution, T = absolute temperature, and A, B, and D = constants. Thermodynamic interpretation of this equation leads to an expression for the true thermodynamic equilibrium constant of $K = m/C_s^A$ and for the enthalpy change, $\Delta H$, of $d \ln(M/C_s^A)/d(1/T) = -\Delta H/R$, where R = universal gas constant.

Experimentally, the sorption of Eu onto clay-rich sediments was very rapid in the first few seconds and slowed over an interval of minutes to hours. Rate curves were similar in shape to those of $\alpha$-iron hydroxide, rather than of the oxalate-extracted residual sediment, indicating the importance of oxyhydroxide-like phases in the uptake of Eu onto red-clay sediments. For clay-rich sediments, numerical modeling reproduced the general features of a series of diffusion experiments. To a first approximation, the penetration of Eu into a sediment proceeded by saturation of the sediment to the depth of penetration and produced a sharp drop-off in sorbed + dissolved Eu concentration at the diffusion front. Higher partition coefficients ($K_p$) resulted in greater sorbed + dissolved concentrations, but reduced penetration. For calcareous sediments, however, Eu concentrations at the surface were much higher than at depth, presumably due to the formation of an insoluble carbonate.

**Key Words**—Deep-sea sediments, Diffusion, Europium, Partition coefficient, Sorption, Thorium.

## INTRODUCTION

Under the U.S. Department of Energy's Subseabed Disposal Program, distribution coefficients for the partitioning of Eu and Th between deep-sea sediments (Tables 1 and 2) and solutions have been determined to evaluate the effectiveness of the sediments as a potential barrier to the migration of radionuclides. The results of these experiments are systematic, but they do not conform readily to the familiar theories of adsorption of Langmuir (for which plotting $\ln(M/C_s)$ against M should give a straight line [Hayward and Trapnell, 1964, p. 1967]), Freundlich (for which plotting $\ln M$ against $RT \cdot \ln(C_s)$ should give a straight line [Hayward and Trapnell, 1964, p. 175]), or Temkin (for which plotting $\ln C_s$ against M should give a straight line [Hayward and Trapnell, 1964, p. 178]). Thus, the fundamental understanding of the sorption process is lacking to predict the effectiveness of sediments as barriers to radionuclide migration, particularly if experimentally determined partition coefficients have to be incorporated in a general model of diffusion. Such a model is necessary because the radionuclides must be held in the sediments for $10^4$ to $10^7$ years in order for them to decay to harmless levels, a period far too long for experimental verification. The model is, of necessity, numerical, because dependence of the partition coefficients on cation concentrations renders an exact solution of the differential equations of diffusion impossible. The problem is further complicated if diffusion through a suite of sediments of variable composition is to be modeled.

Previous models of diffusion in sediments have assumed that the distribution coefficient $K_p$ (ratio of the concentration on the sediment to the concentration in the solution) is constant (Duursma and Hoede, 1967). Heath *et al.* (1977, 1978, 1979) carried out a series of batch sorption experiments to define the dependence of Eu(III) sorption by deep-sea deposits on concentrations, temperature, and sediment type. The results of these experiments indicated that $K_p$ actually varies by orders of magnitude. Application of these results to the diffusion equation suggested by Duursma and Hoede (1967) produces an equation which appears not to have an analytical solution; thus, it must be solved by numerical modeling methods.

A preliminary assessment of the impact of the experimental results on subseabed disposal has been made by estimating diffusion (with sorption) through a sec-

Table 1. Sample locations.

| Sample number | Sediment core | Depth in core (cm) | Latitude | Longitude | Water depth (m) |
|---|---|---|---|---|---|
| T1 | Y74-3-71K | 410–413 | 33°27′N | 150°59′W | 5506 |
| T2 | Y74-3-58P | 867–1083 | 33°10.1′N | 150°54.1′W | 5600 |
| Q1 | Y74-66LG | 20–25 | 33°12.8′N | 150°58.8′W | 5480 |
| GPC2 | LL44-GPC2 | 3000 | 30°20.9′N | 157°50.85′W | 5890 |
| SR1 | JYN-V-28P | — | 14°13′N | 146°24′W | 4952 |
| CN1 | Equatow 27P | — | 7°36.7′N | 134°1.2′W | 4430 |
| GPC3-3 | LL44-GPC3 | 172–182 | 30°19.9′N | 157°49.4′W | 5705 |
| GPC3-4 | LL44-GPC3 | 272–282, 297–307 | 30°19.9′N | 157°49.4′W | 5705 |
| GPC3-13 | LL44-GPC3 | 1610–1620, 1670–1680 | 30°19.9′N | 157°49.4′W | 5705 |
| GPC3-14 | LL44-GPC3 | 1815–1835 | 30°19.9′N | 157°49.4′W | 5705 |

tion of deep-sea red clay recovered in a core collected about 700 nautical miles north of Hawaii at 30°20′N, 157°49′W in a water depth of 5705 m (Corliss *et al.*, 1982; Doyle and Riedel, 1979; Prince *et al.*, 1980). The core (GPC-3) consisted of 10 m of eolian, illite-rich clay, deposited during the last 20 million years (my), overlying 14 m of smectite-rich clay deposited over a period of 50 my. The illite-rich sediment contained illite, kaolinite, chlorite, and smectite in the ratios 24:5:1.3:1 (determined by the method of Heath and Pisias, 1979). The smectite-rich sediment contained the same minerals, but in a typical ratio of 20:10:1:24. Detailed mineralogic profiles of GPC-3 were discussed by Corliss *et al.* (1982) and Leinen and Heath (1981). The area around GPC-3 is not a likely disposal area, but the lithologic section in the core is typical of the pelagic red clays that lie beneath millions of square kilometers of the North Pacific gyre.

## METHODOLOGY

### *Batch sorption experiments*

*Preparation of sediment.* About 1 kg of clay was disaggregated by tumbling with distilled water in a jar mill. One- to two-gram portions of the slurry were split with a wet splitter, placed in dialysis tubing, and dialyzed against distilled water to remove salts. The completeness of salt removal was tested with a $AgNO_3$ solution. The sediment was then removed from the tubing and freeze-dried. The sources of the sediments are shown in Tables 1 and 2.

*Preparation of stock solutions.* Solutions of the selected concentrations were prepared by dissolving appropriate quantities of the chloride salt in distilled water. Aliquots of these solutions were analyzed to determine the exact concentration of the cation, inasmuch as hydroscopic effects make an exact weighing impossible. Thorium was analyzed by oxalate precipitation and ignition (Rodden, 1950). Europium was determined by titration of the chloride by the Mohr method (Kolthoff and Sandell, 1946). Aliquots of these solutions were diluted to the chosen molarities, with the addition of sufficient NaCl to yield an ionic strength of 0.68. An amount of an appropriate radiotracer was added to follow the course of the reactions.

*Exposure of sediments to solution.* Weighed 0.1-g samples were added to preweighed 50-ml polycarbonate centrifuge tubes with screw-cap closures. To obtain the sodium form of the sediment, each sample was dispersed in 25 ml of 0.68 M NaCl solution for 30 min, centrifuged, and the supernatant decanted. This step was repeated two more times. After the final decanting the tube and contents were reweighed to determine the amount of residual chloride solution. Then 25-ml aliquots of the spiked solutions were added to the prepared samples. The sediment was thoroughly dispersed in each tube by shaking, and the capped tubes were placed in constant temperature baths for 18 to 24 hr. The tubes were removed and agitated several times during the first few hours, but allowed to settle overnight. The tubes were centrifuged, and aliquots of the supernatants were removed for gamma counting using a 3-inch sodium iodide detector. The distribution coefficient for the cation (the ratio of its conentration in the sediment to its concentration in the supernatant solution) in each experiment was then determined from the relation:

$$K_p = \frac{rC_0 - C_s}{C_s} \cdot \frac{V}{W}, \quad (1)$$

where: $K_p$ = distribution coefficient (ml/g), V = total volume of solution (25 ml + x residual ml), W = total weight of sediment (g), r = ratio of spike to total solution (25/(25 + x)), $C_0$ = activity (or concentration) of original solution (cpm/ml or mole/liter), and $C_s$ = activity (or concentration) of supernatant solution (cpm/ml or mole/liter). The difficulty of separating the sediment from pore waters necessitated the determination of sorbate concentrations on the sediment by difference from the decrease in supernatant concentrations. Blank and standard solutions without sediment were run through the same procedure, and each experiment was carried out in triplicate. To the precision that results are reported, no corrections for blanks or for sorption of cations onto materials other than sediments were required.

### *Kinetic experiments*

Three methods were employed to investigate the kinetics of the sorption process:

(1) Samples of sediment were exposed to solutions in the same manner as for the batch sorption experiments but allowed to remain in the constant temperature bath for periods of days, then removed, centrifuged, and the supernatant counted. This method is, of course, suitable only for examination of slow reactions.

(2) Sediment was exposed to $EuCl_3$ solution spiked with $^{154}Eu$ in a polycarbonate jar fitted with a magnetic stirring bar on a pivot (to maintain the sediment suspension without grinding the sediment). Aliquots of the suspension were removed periodically and filtered, and the filtrate was counted to determine the Eu concentration in the liquid phase of the suspension. Volumes of solution of 200–250 ml and weights of sediment suitable to maintain the same ratio as in the batch sorption experiments (0.1 g to 25 ml) were used. Although

Table 2. Sample depths in core LL44-GPC3.

| Sample number | Depth in core (m) | Sample number | Depth in core (m) |
|---|---|---|---|
| 2 | 58–68 + 77–87 | 11 | 1314–1338 |
| 3 | 172–182 | 12 | 1501–1521 |
| 4 | 272–282 + 297–307 | 13 | 1610–1620 + 1670–1680 |
| 5 | 387–397 + 422–432 | 14 | 1815–1835 |
| 6 | 540–550 + 580–590 | 15 | 1920–1940 |
| 7 | 690–710 | 16 | 2055–2075 |
| 8 | 832–842 + 849–859 | 17 | 2191–2201 + 2211–2221 |
| 9 | 1045–1065 | 18 | 2365–2385 |
| 10 | 1157–1167 + 1187–1197 | 19 | 2435–2455 (flow-in) |

aliquots could be withdrawn at intervals of less than 1 min, resolution was lost because of the time necessary to filter each aliquot of suspension (on the order of 5–10 s).

(3) Differential pulse polarography with a dropping mercury electrode was employed in an attempt to determine the Eu concentration in the liquid phase of suspensions as the sorption process was taking place. Volumes of 12.5 ml of solutions of $EuCl_3$ with a supporting electrolyte 0.68 M in NaCl were deoxygenated by bubbling nitrogen through them and loaded with 50 mg of sediment (again maintaining the same ratio as in the batch sorption experiments). Polarographic scans were then made periodically. Determinations made on standard solutions indicated linear response of the instrument to Eu concentration and no detectable deviations due to variations in pH.

To separate effects due to surface coatings from those involving silicate structures, samples of sediment were treated with ammonium oxalate to remove noncrystalline iron and aluminum oxides. For comparison, experiments were also carried out with noncrystalline $\alpha$-iron hydroxide.

*Diffusion experiments*

Samples of the sediments prepared for the column sorption experiments were weighed into 50-ml polycarbonate centrifuge tubes and reconstituted to the approximate bulk density of the freshly recovered sediments. The tubes were then cut off just above the surfaces of the sediments and placed in a reservoir bath containing 14 liters of a solution 0.002 M in $EuCl_3$ doped with $^{154}Eu$, made up to an ionic strength of 0.68 with NaCl, and held at 85°C by means of a hot water bath. Three 5-ml aliquots of the solution were removed periodically (generally every day during the work week) and counted. Aliquots of the spiked $EuCl_3$ solution and the NaCl solution were added to maintain the concentration and volume of the solution, and aliquots of the solution were taken after each addition to ensure that the additions had been properly made. The tubes were removed from the reservoir after 109 days, and penetration of Eu into the tubes was determined by scanning each tube through a 7-mm slit between two lead bricks behind which was a Geiger tube attacked to a counter. The sample tubes were moved by means of spacers, and a 1-min count was taken at each depth in the sediment. Background counts were taken as well. The instrument was calibrated using T2 sediment (Table 1). A sample of the top surface of this sediment was placed in a weighed centrifuge tube and air dried; it was then weighed and treated with a 25-ml aliquot of 20% HCl, vortexed, and allowed to settle overnight. The tube was then centrifuged, and three 5-ml aliquots of the supernatant were taken and counted to yield the amount of Eu on the weighed portion of sediment. From the bulk density of the *in situ* sediment and the amount of Eu on the weighed portion of sediment, the volume concentration of Eu in the surface sediment was calculated. By assuming that the highest count obtained during the passage of this sediment column in front of the Geiger tube represented the concentration of Eu at its surface, the bulk concentration of Eu at each point along each sediment column could be estimated by ratioing to this value.

## RESULTS AND DISCUSSION

*Batch sorption experiments*

The results of all deep-sea clay, Eu-sorption experiments are summarized in Figure 1. At very low Eu(III)

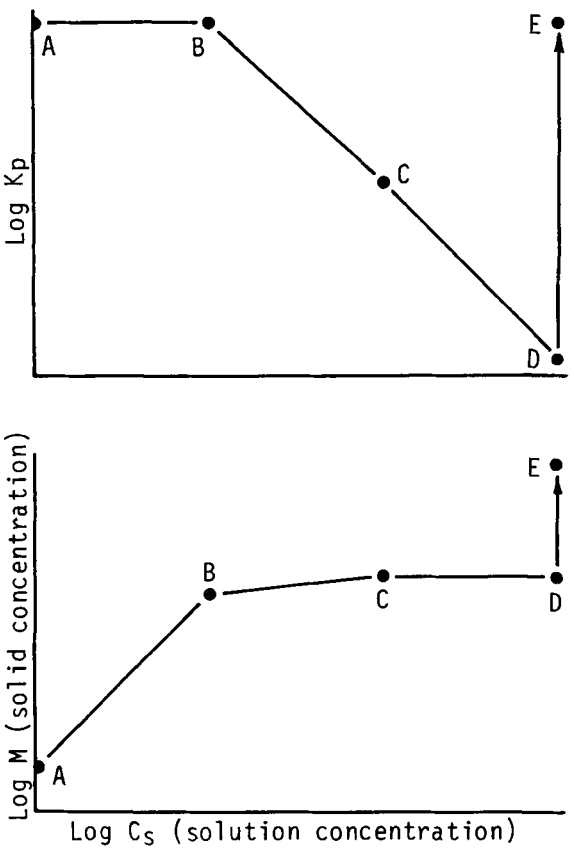


Figure 1. Generalized behavior of solid phase concentration (M) and partition coefficient ($K_p = M/C_s$) as a function of dissolved concentration ($C_s$) for Th and Eu. See text for explanation.

https://doi.org/10.1346/CCMN.1986.0340310 Published online by Cambridge University Press

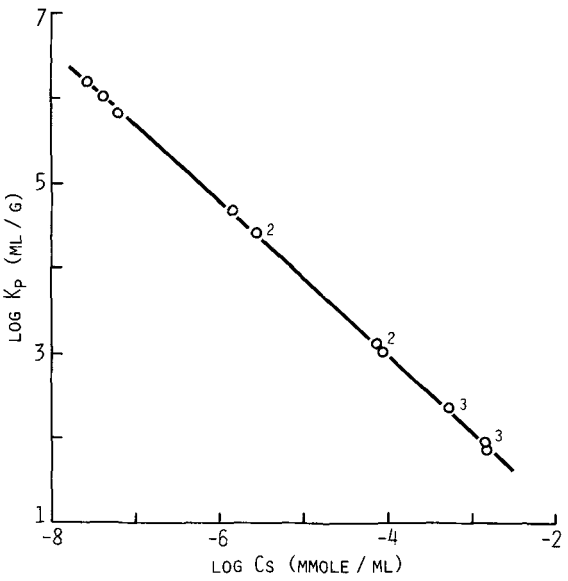


Figure 2. Sorption of Eu from 0.68 M NaCl at 15°C by smectitic clay T2. $C_s$ in mM/ml, $K_p$ in ml/g. Numbers = number of measurements covered by the plotted data point.

Table 3. Estimates of the thermodynamic equilibrium constant (K) for the sorption of Eu(III) from 0.68 M NaCl solutions at 15°C onto T2 sediment.

| | | $K = M/C_s^{0.1047}$ | | |
|---|---|---|---|---|
| $C_o$ (mmole/ml) | $C_s$ (mmole/ml) | M (mmole/ 100 g) | K | Mean K |
| 0.002 | $1.46 \times 10^{-3}$ | 12.3 | 24.4 | |
| | $1.44 \times 10^{-3}$ | 12.9 | 25.6 | |
| | $1.50 \times 10^{-3}$ | 11.6 | 22.9 | 24.3 ± 1.4 |
| 0.001 | $5.01 \times 10^{-4}$ | 11.8 | 26.2 | |
| | $5.36 \times 10^{-4}$ | 12.4 | 27.3 | |
| | $5.23 \times 10^{-4}$ | 12.2 | 26.9 | 26.8 ± 0.6 |
| 0.0005 | $7.63 \times 10^{-5}$ | 10.4 | 28.1 | |
| | $8.46 \times 10^{-5}$ | 9.23 | 24.6 | |
| | $7.13 \times 10^{-5}$ | 9.66 | 26.3 | 26.3 ± 1.8 |
| 0.0003 | $2.64 \times 10^{-6}$ | 6.76 | 25.9 | |
| | $1.42 \times 10^{-6}$ | 6.99 | 28.6 | |
| | $2.79 \times 10^{-6}$ | 7.38 | 28.2 | 27.6 ± 1.5 |
| 0.0002 | $2.71 \times 10^{-8}$ | 4.26 | 26.4 | |
| | $6.20 \times 10^{-8}$ | 4.10 | 23.3 | |
| | $3.99 \times 10^{-8}$ | 4.14 | 24.6 | 24.8 ± 1.6 |
| | | Mean 26.0 ± 1.7 | | |

concentrations ($<10^{-8}$ M), $K_p$ was constant or $M \propto C_s$ (A to B in Figure 1). Between B and C (Figure 1) $K_p \propto C_s^{-0.9}$ (approximately), or $M \propto C_s^{0.1}$. At point C, the clay was saturated, so that from C to D, M was constant and $K_p \propto 1/C_s$. From D to E, the solution was saturated, and a Eu(III) phase began to precipitate.

The data between B and C (Figure 1) may be represented by an equation of the form:

$$\ln M = A \ln C_s + B/T + D, \quad (2)$$

where M = concentration of sorbate on sediment, $C_s$ = concentration of sorbate in solution, T = absolute temperature, and A, B, and D = constants. Application to Eq. (2) of the Clausius-Clapeyron equation (which strictly applies only to sorption of gases) gives:

$$q = R(d \ln C_s/d(1/T))M, \quad (3)$$

where q = energy of sorption and R = universal gas constant, suggesting the relationship:

$$\ln M = A \ln C_s - (q \cdot A)/RT + D. \quad (4)$$

A comparison of Eq. (4) with the integrated form of the van't Hoff equation,

$$\ln K = -\Delta H/RT + \text{const.}, \quad (5)$$

where K = true thermodynamic equilibrium constant and $\Delta H$ = enthalpy change (assumed constant), further suggests that the true thermodynamic equilibrium constant is given by:

$$K = M/C_s^A. \quad (6)$$

Applying van't Hoff's equation:

$$d(\ln K)/d(1/T) = -\Delta H/R \quad (7)$$

to Eq. (2) yields:

$$d \ln(M/C_s^A)/d(1/T) = -\Delta H/R. \quad (8)$$

Further, $\Delta G$, the free energy change, and $\Delta S$, the entropy change, are given by:

$$\Delta G = -RT \ln K \quad (9)$$

and

$$\Delta G = \Delta H - T\Delta S. \quad (10)$$

Figure 2 shows $\log K_p$ vs. $\log C_s$ for sorption of Eu(III) from 0.68 M NaCl solutions at 15°C onto a smectite-rich sediment from the North Pacific (T2). Regressing $\log K_p$ against $\log C_s$ and solving for K from $K = M/C_s^A$ gives the relationship $K = M/C_s^{0.1047}$. Values of K derived from this relationship (Table 3) are remarkably constant over five orders of magnitude of $C_s$. The reason for the extreme insensitivity of M to variations in $C_s$ is unknown. The activity of sorbate associated with the solid phase is nearly independent of $C_s$, similar to a precipitation reaction. Thus, the solution chemistry must play a more important role than the surface chemistry in the sorption process. McBride (1980) suggested that such processes are driven by entropy increases during sorption that are caused by the loss of ordered water of hydration from multiply-charged ions in solution.

Figure 3 shows the temperature dependence of the $\log K_p$ vs. $\log C_s$ regression for the sorption of Th from 0.68 M NaCl solutions onto an illite-rich sediment from the North Pacific (Q1). The calculation of $\Delta H$ by regression of $\log K_p$ against $\log C_s$ and 1/T based on

https://doi.org/10.1346/CCMN.1986.0340310 Published online by Cambridge University Press

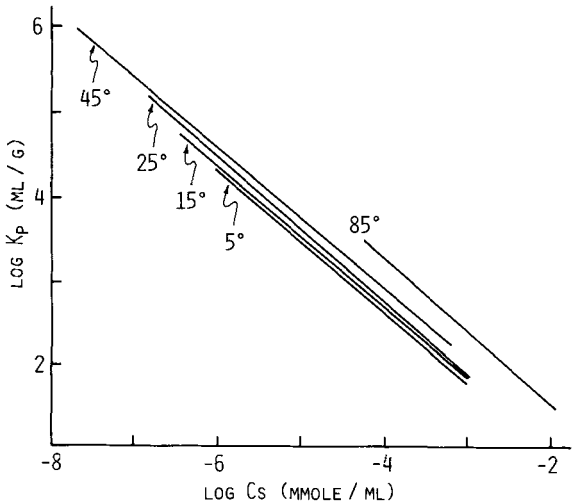


Figure 3. Temperature dependence of the sorption of Th from 0.68 M NaCl by illitic clay Q1. $C_s$ in mM/ml, $K_p$ in ml/g.

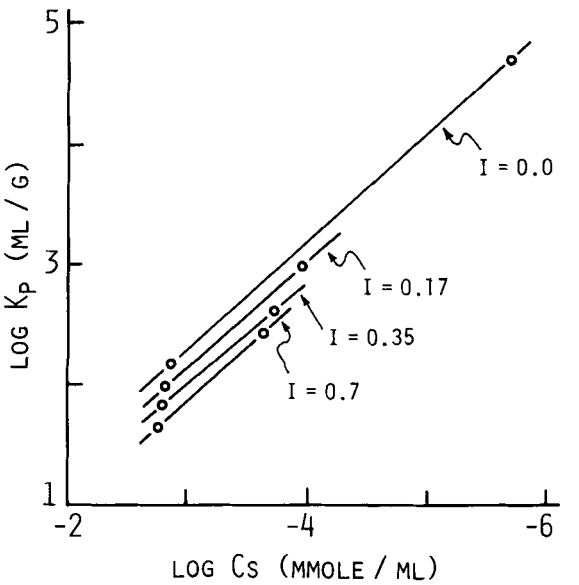


Figure 4. Dependence of the sorption of Eu on smectitic clay T1 at 85°C on the ionic strength of matrix NaCl solutions. $C_s$ in mM/ml, $K_p$ in ml/g.

Eq. (2) yielded the small ΔH of 3.83 kcal/mole (Appendix I), which is typical of sorption phenomena (Hayward and Trapnell, 1964, 194–225). The ΔH was positive, which implies increased sorption with increased temperature, as seen from examination of the van't Hoff equation. For comparison, Laudelout *et al.* (1968) determined enthalpy values of 1.30 kcal/mole for Mg replacement of Na on Camp Berteau montmorillonite, and 1.22 kcal/mole for Ca replacement of Na. For the strongly sorbing smectite sediment T2, the temperature dependence was less than for the less highly sorbing Q1 sediment, but regression of log $K_p$ against log $C_s$ and 1/T again gave a high correlation coefficient of .9947 and yielded a ΔH value of 1.66 kcal/mole (Appendix II), which is less than half of that for the Q1 sediment, indicating that sorption increased less rapidly with temperature than it did for the Q1 sediment.

Figure 4 shows log $K_p$ vs. log $C_s$ trends for the sorption of Eu(III) from NaCl solutions of various ionic strengths at 85°C onto the T1 sediment. Regressing log $K_p$ against log $C_s$ and log(NaCl) and solving for K (Appendix III) gave the relationship:

$$K = \frac{(M)(NaCl)^{0.3978}}{C_s^{0.1273}} = 0.1552. \qquad (11)$$

The term $(NaCl)^{0.3978}$ suggests that although NaCl was sorbed less strongly than Eu(III), it did indeed compete with Eu(III) for sorption sites on the sediment.

*Rate experiments*

Figure 5 shows sequential polarograms of sorption of Eu from solutions $5 \times 10^{-4}$ M in $EuCl_3$ and 0.68 M in NaCl onto the T2 sediment. Figure 6 shows the decline in supernatant Eu concentration for oxalate-extracted T2 sediment and noncrystalline α-iron hydroxide, as well as for the T2 sediment with time. It also includes a curve for the T2 sediment determined by the method of removing aliquots using $^{154}Eu$ tracer (29°C curve). Sorption onto the oxalate-extracted sediment was quite different from sorption onto either the T2 sediment or the α-iron hydroxide, which were similar in shape. Note, however, that for all samples, sorption during the initial few seconds was very rapid, and became slower over an interval of minutes to hours (Table 4). Figure 7 shows the data plotted such that linear portions indicate first-order kinetics (Glasstone, 1946). No convincing conformity with first order kinetics is apparent. What is evident from Figure 7 is that sorption onto the untreated T2 sediment was similar to sorption onto α-iron hydroxide, but not onto its own oxalate-extracted residual material. Figure 8 shows the data for the T2 sediment and α-iron hydroxide plotted such that linear portions indicate diffusion into a crystal structure (Palmer and Bauer, 1961). It is evident that no such diffusion took place. Figure 9 shows the same kind of plot for the oxalate-extracted T2 sediment. Here, the two linear portions imply that two processes of diffusion into the crystal lattice were at work. The reasons for the change from a slower to a more rapid rate is unknown, but may have resulted from expansion of the phyllosilicate structures to the point where Eu(III) entered structural sites.

These results suggest that for sorption reactions occurring in hours or less, oxyhydroxide-like phases (possibly grain coatings) played an important role in the uptake of Eu onto deep-sea clay sediments.

https://doi.org/10.1346/CCMN.1986.0340310 Published online by Cambridge University Press

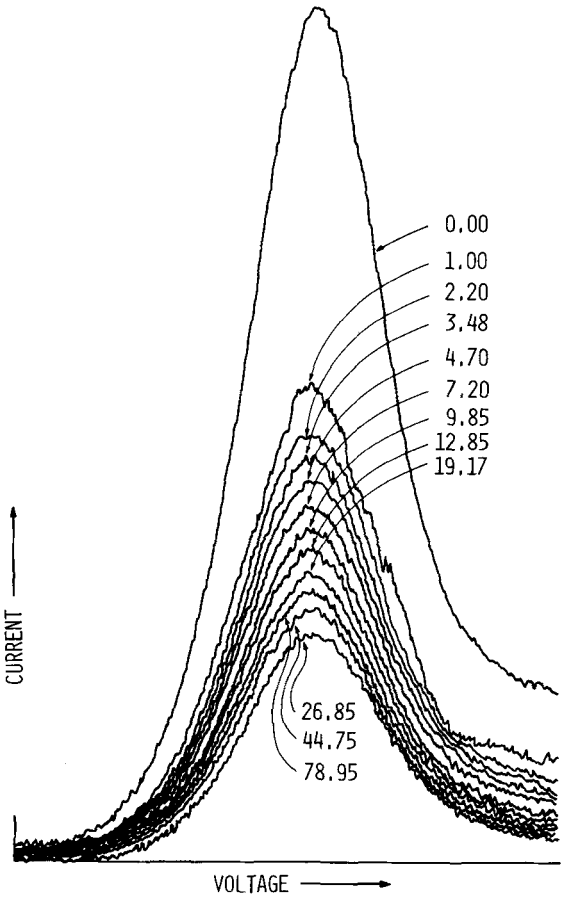


Figure 5. Sequential polarograms of Eu removal from 12.5 ml of solution initially at $5 \times 10^{-4}$ M in Eu and 0.68 M in NaCl by 50 mg of smectitic clay T1. Numbers = minutes from the start of the experiment.

*Diffusion model*

The equations of fluid dynamics apply strictly and rigorously to the diffusion of an ion in the pore waters of a sediment. To model the transport of an ion in the bulk sediment, we interpreted diffusion in the pore waters in terms of the bulk sediment. The diffusion of an ion subject to sorption in sediments was given by Duursma and Hoede (1967) as

$$\frac{\partial C}{\partial t} + \frac{\partial KdC}{\partial t} = D \cdot \frac{\partial^2 C}{\partial x^2}, \qquad (12)$$

in which the term $\frac{\partial KdC}{\partial t}$ treats the sediment as a source or a sink of the ion. We additionally took into account the tortuous path an ion must take in moving through the pore waters of the sediment and expressed all equations in terms of bulk properties of the sediment. In cylindrical coordinates:

$$\frac{\partial C_b'}{\partial t} = \frac{D}{F}\left[\frac{\partial^2 C}{\partial z^2} + \frac{1}{r} \cdot \frac{\partial}{\partial r}\left(r \cdot \frac{\partial C}{\partial r}\right)\right], \qquad (13)$$

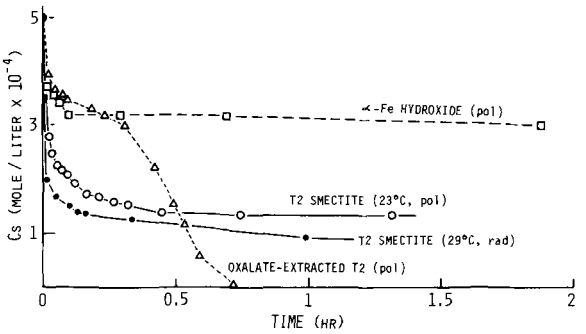


Figure 6. Eu concentration of supernate as a function of time during sorption by smectitic clay T2 (pol = polarography, rad = radiotracer), by its residue after oxalate extraction, and by α-iron hydroxide.

where C = pore water concentration, $C_b$ = concentration in sediment, D = free diffusion coefficient, F = formation factor, Kd = volume distribution coefficient = $Mv/C_s$, with Mv and $C_s$ in volume units (e.g., Mv and $C_s$ in mmole/ml), where Mv = mmole of sorbate on sediment/ml of bulk sediment, z = downcore depth, and r = radial distance orthogonal to z. Note that:

$$\begin{aligned} C_b' &= C + \rho/\epsilon \cdot K_p \cdot C, \\ C_b' &= C(1 + \rho/\epsilon \cdot K_p), \\ C_b' &\sim C \cdot \rho/\epsilon \cdot K_p, \text{ and} \\ C_b' &\sim C_b/\epsilon, \end{aligned} \qquad (14)$$

where $\rho$ = bulk density, $\epsilon$ = porosity, and $K_p$ = partition coefficient (ml/g). Based on Li and Gregory's (1974) data for La(III) and the Arrhenius equation:

$$D = D_0 e^{-E/RT}, \qquad (15)$$

D is given by:

$$\ln D = -2.618 \times 10^3 \left(\frac{1}{T}\right) - 3.21135 \quad (D \text{ in } cm^2/s), \qquad (16)$$

as suggested by Manheim (1970). The formation factor F measures the tortuous path that a diffusing species must take in getting through the sediment. F is determined as the ratio of the conductivity of the "free" pore water to the conductivity of the sediment. For sediment-core GPC-3, values of F were determined by R. McDuff (in Corliss *et al.*, 1982) and values of $K_p$ in the form:

Table 4. Uptake of Eu(III) by T2 sediment, the oxalate-extracted residue of T2 sediment, and α-iron hydroxide.

| Sediment | Technique | Initial rate (mmol/100 g/min) | Time for sorption of half of Eu (min) |
|---|---|---|---|
| T2 | Radiotracer | 2.46 | 0.84 |
| T2 | Polarography | 5.29 | 2.67 |
| Ox-Ex-T2 | Polarography | 3.42 | 23.5 |
| α-iron hyd. | Polarography | 3.51 | >113 |

https://doi.org/10.1346/CCMN.1986.0340310 Published online by Cambridge University Press

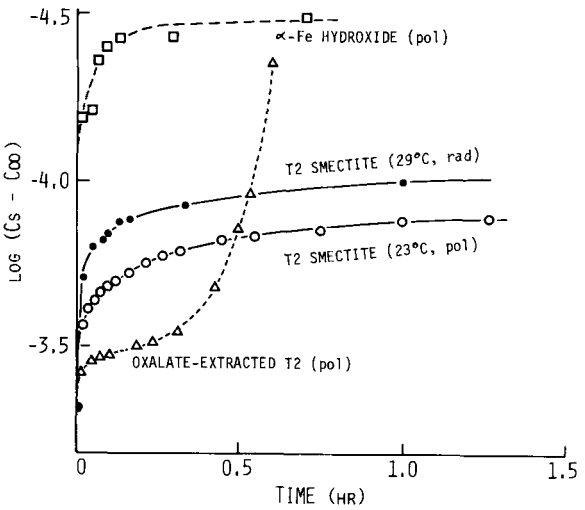


Figure 7. $\text{Log}(C_s - C_\infty)$ of Eu in the supernate as a function of time during sorption by the phases of Figure 6.

$$\log K_p = A' \log C + B', \qquad (17)$$

by G. B. Epstein and D. Walsh (see Heath *et al.*, 1977, 1978, 1979).

The diffusion column experiments were modeled using the one-dimensional case of Eq. (13) in numerical form (Roache, 1972):

$$C'^{n+1}_b = \frac{D}{F}\left(\frac{C^n_{i+1} + C^n_{i-1} - 2C^n_i}{(\Delta x^2)}\right)\Delta t + C'^n_b, \qquad (18)$$

where the differentials have been replaced by their numerical approximations (derived from Taylor series), in which n increments time and i increments z, and

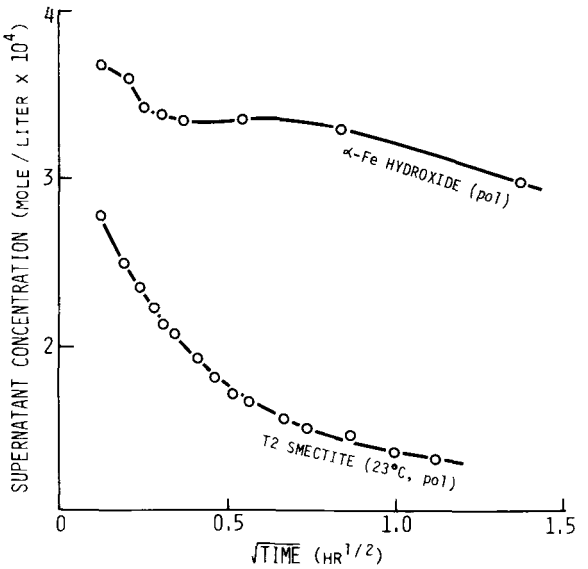


Figure 8. Eu concentration of supernate as a function of $(\text{time})^{1/2}$ during sorption by smectitic clay T2 and by $\alpha$-iron hydroxide.

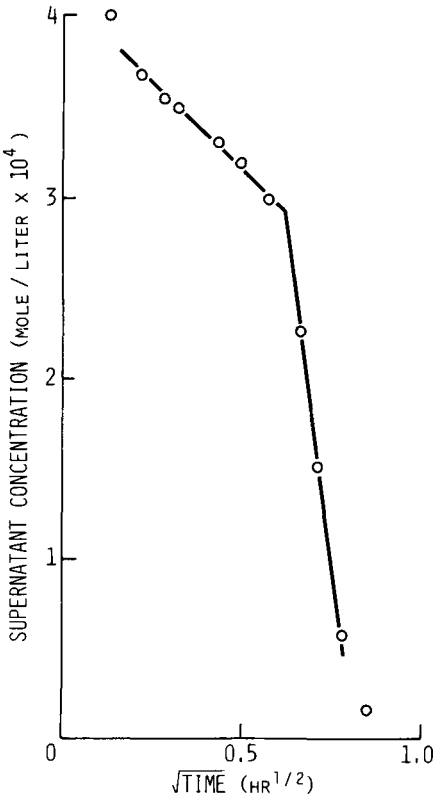


Figure 9. Eu concentration of supernate as a function of $(\text{time})^{1/2}$ during sorption by oxalate-extracted smectitic clay T2.

from which $C'^{n+1}_b$ can be calculated using Eqs. (14) and (17).

To model one-dimensional diffusion into a composite sediment (GPC3-10 and GPC3-11) which had sorption properties that were a gross average of those of the sediments placed in the constant-composition solution, values of $\epsilon = 0.80$, $\rho/\epsilon = 0.505$, $F = 4.37$, and $K_p = 0.494C_s^{-0.876}$ were used. Figure 10 shows the results of the model calculation. If the concentration of the solution varies by $\pm 5\%$ via a sawtooth function within a period of 4 days in the same model, to approximate more closely the actual variation of the concentration of the Eu solution, the calculated Eu concentration of the pore solutions is affected to a shallow

Table 5. Formation factor F used to estimate model grid point values.

| Depth in core (cm) | F |
|---|---|
| 0–439 | 3.98 |
| 449–618 | 4.47 |
| 716–927 | 4.57 |
| 1007–1223 | 3.80 |
| 1316–1832 | 4.37 |
| 1902–2075 | 5.25 |
| 2120–2399 | 5.62 |

https://doi.org/10.1346/CCMN.1986.0340310 Published online by Cambridge University Press

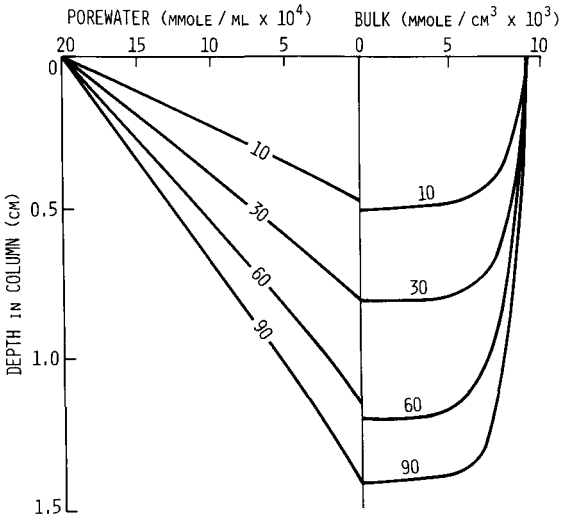


Figure 10. Modeled one-dimensional diffusion of Eu in 0.68 M NaCl solution at 85°C into smectitic clay with the properties of sample GPC3-10/11.

depth, but the bulk concentration is unaffected. In Figure 11, the total amount of sorption from the solution as a function of elapsed time was calculated from the areas under the bulk-concentration curves of Figure 10. This curve was scaled to allow its shape to be compared with that of the experimental curve. The agreement is satisfactory, particularly because the sediments in the model were not exactly equivalent to those in the tank.

To provide a crude illustration of the effect of downcore variations in sediment properties on Eu(III) dif-

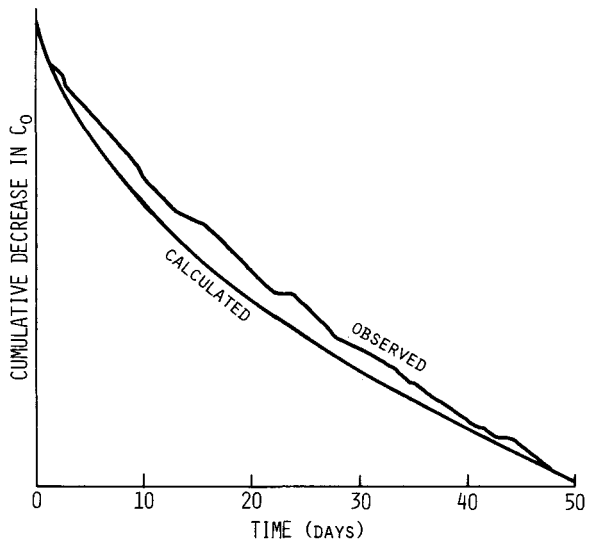


Figure 11. Estimated and observed cumulative uptake of Eu during column experiment based on sorption properties of sample GPC3-10/11.

Table 6. Data used to estimate grid-point values of bulk density ($\rho$) and porosity ($\epsilon$).

| Depth in core (cm) | Water content (% dry weight) | Particle density ($g/cm^3$) | Porosity ($cm^3/cm^3$) |
|---|---|---|---|
| 0 | 124 | 2.70 | 0.770 |
| 39 | 118 | 2.80 | 0.770 |
| 78 | 117 | 2.78 | 0.766 |
| 117 | 194 | 2.83 | 0.846 |
| 156 | 108 | 2.87 | 0.757 |
| 195 | 105 | 2.77 | 0.743 |
| 234 | 105 | 2.88 | 0.751 |
| 273 | 107 | 2.91 | 0.757 |
| 312 | 110 | 2.88 | 0.759 |
| 351 | 108 | 2.86 | 0.766 |
| 390 | 105 | 2.96 | 0.757 |
| 429 | 105 | 2.85 | 0.749 |
| 468 | 110 | 2.82 | 0.757 |
| 507 | 111 | 2.78 | 0.755 |
| 546 | 120 | 2.76 | 0.768 |
| 585 | 110 | 2.80 | 0.755 |
| 624 | 111 | 2.85 | 0.760 |
| 663 | 117 | 2.83 | 0.769 |
| 702 | 134 | 3.12 | 0.806 |
| 741 | 146 | 2.81 | 0.804 |
| 780 | 156 | 2.93 | 0.821 |
| 819 | 166 | 2.78 | 0.822 |
| 858 | 158 | 2.78 | 0.814 |
| 897 | 176 | 3.02 | 0.842 |
| 936 | 181 | 3.00 | 0.844 |
| 975 | 175 | 2.92 | 0.836 |
| 1014 | 167 | 2.73 | 0.820 |
| 1053 | 201 | 2.83 | 0.850 |
| 1092 | 208 | 2.87 | 0.856 |
| 1131 | 231 | 2.82 | 0.867 |
| 1170 | 253 | 2.89 | 0.880 |
| 1209 | 209 | 2.98 | 0.861 |
| 1248 | 211 | 2.79 | 0.855 |
| 1326 | 233 | 2.84 | 0.869 |
| 1404 | 225 | 2.91 | 0.867 |
| 1443 | 221 | 2.85 | 0.863 |
| 1482 | 240 | 2.79 | 0.870 |
| 1521 | 240 | 2.86 | 0.873 |
| 1560 | 211 | 3.03 | 0.865 |
| 1599 | 224 | 3.03 | 0.872 |
| 1638 | 212 | 2.91 | 0.860 |
| 1677 | 215 | 2.85 | 0.860 |
| 1716 | 201 | 3.07 | 0.861 |
| 1755 | 195 | 2.97 | 0.853 |
| 1794 | 202 | 2.52 | 0.836 |
| 1833 | 203 | 1.67 | 0.772 |
| 1872 | 215 | 2.78 | 0.857 |
| 1911 | 233 | 2.70 | 0.863 |
| 1950 | 218 | 2.68 | 0.854 |
| 1989 | 229 | 2.75 | 0.863 |
| 2028 | 176 | 2.67 | 0.824 |
| 2067 | 179 | 2.75 | 0.831 |
| 2106 | 205 | 2.73 | 0.848 |
| 2145 | 200 | 2.79 | 0.848 |
| 2184 | 176 | 2.71 | 0.827 |
| 2223 | 195 | 2.78 | 0.844 |
| 2262 | 212 | 2.88 | 0.859 |
| 2301 | 185 | 2.81 | 0.838 |
| 2340 | 164 | 2.68 | 0.815 |
| 2379 | 160 | 2.84 | 0.820 |
| 2425 | 147 | 2.84 | 0.807 |
| 2457 | 163 | 2.84 | 0.823 |

https://doi.org/10.1346/CCMN.1986.0340310 Published online by Cambridge University Press

Table 7. Constants of the equation $\log K_p = A' \log C + B'$ for sorption of Eu by core LL44-GPC3 used to estimate grid point values of A' and B'.

| Sample | 15°C | | 85°C | |
|---|---|---|---|---|
| | A' | B' | A' | B' |
| 2 | −0.835 | −1.149 | −0.890 | −0.915 |
| 3 | −0.692 | −0.713 | −0.798 | −0.680 |
| 4 | −0.745 | −0.894 | −1.063 | −1.635 |
| 5 | −0.770 | −0.970 | −0.870 | −0.933 |
| 6 | −0.749 | −0.818 | −1.101 | −1.680 |
| 7 | −0.808 | −0.863 | −0.923 | −0.993 |
| 8 | −0.800 | −0.674 | −0.929 | −0.859 |
| 9 | −0.822 | −0.546 | −0.922 | −0.597 |
| 10 | −0.859 | −0.730 | −0.894 | −0.652 |
| 11 | −0.833 | −0.532 | −0.817 | −0.240 |
| 12 | −0.837 | −0.523 | −0.777 | −0.091 |
| 13 | −0.877 | −0.575 | −0.904 | −0.432 |
| 14 | −0.841 | −0.490 | −0.908 | −0.496 |
| 15 | −0.832 | −0.614 | −0.874 | −0.544 |
| 16 | −0.800 | −0.722 | −0.835 | −0.556 |
| 17 | −0.823 | −0.684 | −0.924 | −0.763 |
| 18 | −0.751 | −0.550 | −0.820 | −0.517 |
| 19 | −0.758 | −0.593 | −0.848 | −0.597 |

fusion, the GPC-3 section was scaled to 5 cm from its actual length of 25 m. The grid point values of parameters used in the model were interpolated from the values in Tables 5–7. Figure 12 is the model profile for diffusion at 15°C. Model results for 85°C are shown in Figure 13. In this core, Kd values at a number of points between 0.2 and 0.4 cm were modified to adjacent values to avoid irreversible saturation of the sediment, which prevents calculation of C from $C_b$. The model shows that the increase in $K_p$ due to a temperature increase from 15° to 85°C increased the amount of sorption, thereby decreasing the penetration into the sediment, despite the temperature induced increase in D given by Eq. (16).

All of model curves show that the bulk concentration in the sediment increased and approached asymptotically a value given by $C_b = C_0 \cdot K_p \cdot \rho$, where $K_p$ is the

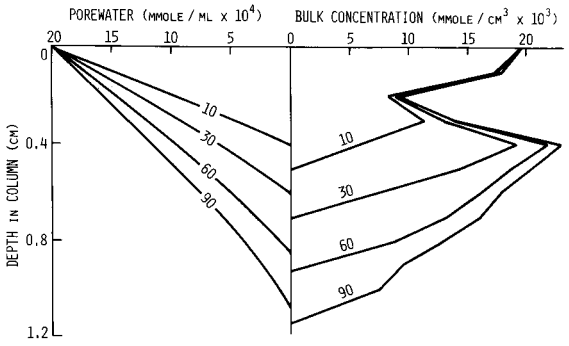


Figure 12. Modeled, one-dimensional diffusion of Eu in 0.68 M NaCl at 15°C into a 1/500 scale section of GPC-3 sediments.

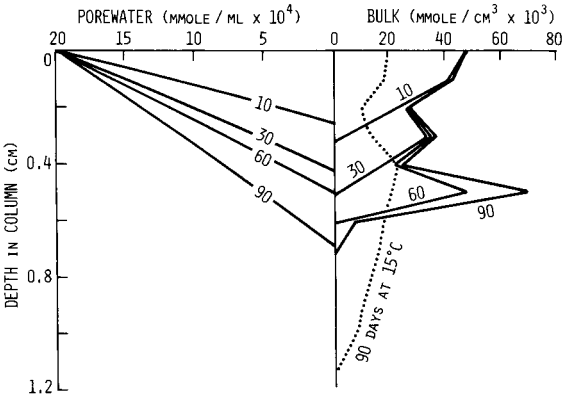


Figure 13. Modeled, one-dimensional diffusion of Eu in 0.68 M NaCl at 85°C into a 1/500 scale section of GPC-3 sediments.

distribution coefficient for $C = C_0$. In other words, to a first approximation, the depth of penetration of Eu can be determined by dividing the amount of Eu by the equilibrium sorption capacity of the sediment for Eu at the initial Eu concentration.

Eq. (13) was used in the difference form

$$C^{n+1}_{b\,i,j} = \frac{D}{F}\cdot\left(\frac{C^n_{i+1,j} + C^n_{i-1,j} - 2C^n_{i,j}}{(\Delta z)^2} + \frac{1}{r}\cdot\frac{C^n_{i+1,j} + C^n_{i,j-1}}{2\Delta r} + \frac{C^n_{1,j+1} + C^n_{i,j-1} - 2C^n_{i,j}}{(\Delta r)^2}\right)\Delta t + C^n_{b\,i,j,} \quad (19)$$

where n = time increment, i = z increment, and j = r increment, to assess the diffusion of 1 $\mu$M Eu from a 2-m long line source parallel to z, and centered at z = 12.5 m in the GPC-3 core. Detectable Eu would move radially only 1.5 m in one million years in the red clay suite of sediments. The radial distribution of concentration was similar to Figure 10, with the same sharp drop-off in bulk concentration at the diffusion front.

The models must of necessity extrapolate to infinite dilution. The basis for such an extrapolation was provided by a physical chemical examination of the batch sorption data, but some of the data still had to be adjusted to keep the model from failing, particularly for highly sorbing sediments at higher temperatures. Further examination of sorption under extreme conditions was thus indicated. The model also used one-day exposure values of $K_p$. Because the sediments were exposed for extended periods of time during diffusion, an examination of the effect on the model of using $K_p$ values derived from longer exposure times would be useful; the results cited here are certainly conservative.

*Diffusion experiments*

Measured values for the bulk concentration of Eu in the experimental sediment column are shown in Fig-

https://doi.org/10.1346/CCMN.1986.0340310 Published online by Cambridge University Press

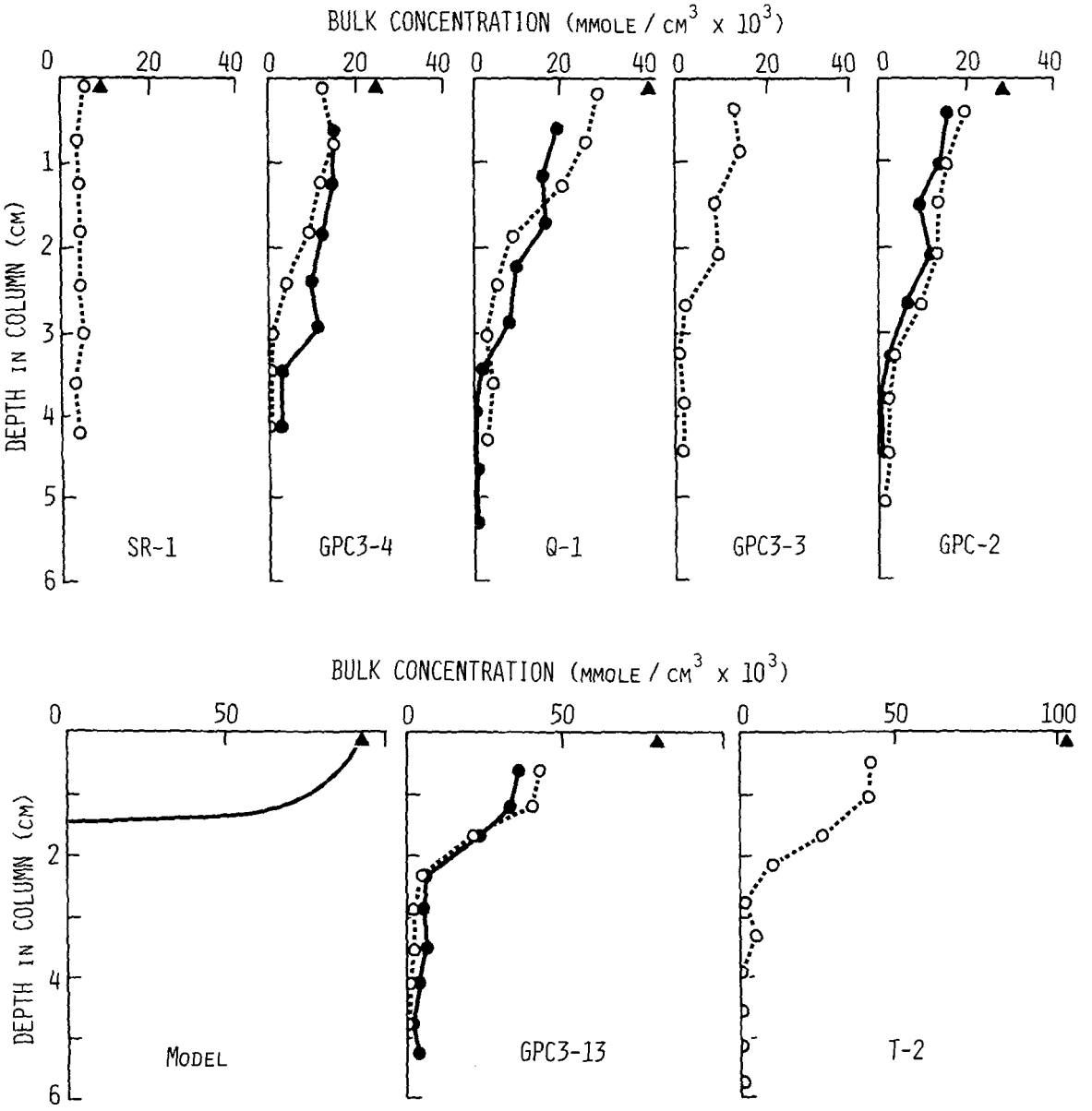


Figure 14. Bulk Eu concentrations in sediment columns after exposure to 0.002 M Eu in 0.68 M NaCl at 85°C for 109 days. Open and closed symbols are for duplicate columns. Counting errors (1 $\sigma$) lie within symbols. Triangles show calculated surface values, based on batch $K_p$ determinations. "Model" is 90-day GPC3-10/11 calculation from Figure 10.

ures 14 and 15. For clay-rich sediments, the results are consistent with those obtained from the numerical model, and in particular:

(1) Penetration was only a few centimeters. Measured values were greater than predicted by the model due to transverse cracks produced in the sediment by degassing of air from the pore waters on heating to 85°C.

(2) Higher $K_p$ values resulted in greater bulk concentrations but reduced penetration.

The simple diffusion model did not work for calcareous sediments. Although batch $K_p$ values for calcareous sediments were in the range of clay values, the surface bulk concentration of Eu in the column experiments (Figure 15) was five times greater than the largest value found for any clay, presumably due to the formation of an insoluble carbonate.

## CONCLUSIONS

### *Batch sorption experiments*

All the data for the sorption of Eu and Th by deep-sea sediments may be represented by equations of the form:

https://doi.org/10.1346/CCMN.1986.0340310 Published online by Cambridge University Press

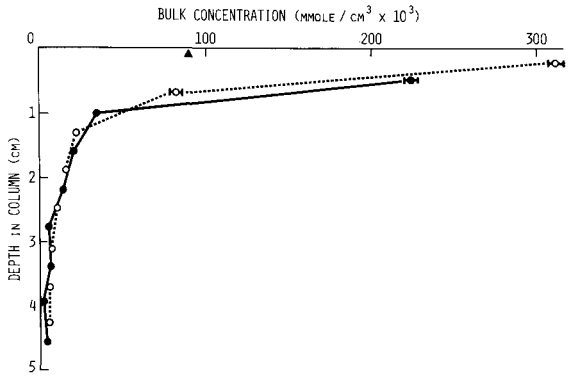


Figure 15. As Figure 14 for carbonate-rich sediment CN1. Counting errors (1 $\sigma$) lie within symbols unless shown by bars.

$$\ln M = A \ln C_s + B/T + D. \quad (2)$$

Thermodynamic interpretation of this equation leads to an expression for the true thermodynamic equilibrium constant:

$$K = M/C_s^A, \quad (6)$$

and for the enthalpy change:

$$d \ln(M/C_s^A)/d(1/T) = -\Delta H/R. \quad (8)$$

*Rates*

Sorption of Eu onto clay-rich sediments was very rapid in the first few seconds and became slower over an interval of minutes to hours. Rate curves were similar in shape to those of $\alpha$-iron hydroxide, rather than those of oxalate-extracted residual sediment, indicating the importance of oxyhydroxide-like phases in the uptake of Eu onto oxidized deep-sea (red) clay sediments.

*Numerical modeling of diffusion experiments*

Numerical modeling reproduced the general features of the diffusion experiments. To a first approximation, penetration of Eu into a sediment proceeded by saturating the sediment to the depth of penetration, thereby producing a sharp drop-off in sorbed + dissolved concentration at the diffusion front. Higher $K_p$ values resulted in greater sorbed + dissolved concentration but reduced penetration. For calcareous sediments, surface sorbed + dissolved Eu concentrations were greater than predicted from batch sorption experiments, presumably due to the formation of an insoluble carbonate.

## ACKNOWLEDGMENTS

We are grateful to David Walsh, for help with the experimental work, and to Dana Kester, F. T. Manheim, and F. A. Mumpton for comments on the manuscript. This research was supported by Sandia National Laboratories contracts 05-7893, 13-2558, and 46-1518.

## REFERENCES

Corliss, B. H., Hollister, C. D., Von Herzen, B., Richardson, M. J., Dow, W., Heath, G. R., Laine, E. P., Prince, R., Epstein, G. B., Leinen, M., Doyle, P., Riedel, W., McDuff, R., Silva, A., Calnan, D., Baldwin, K., Hayes, D., Tucholke, B. E., and Taft, B. (1982) A paleoenvironmental model for Cenozoic sedimentation in the central North Pacific: in *The Ocean Floor,* R. A. Scrutton and M. Talwani, eds., Wiley, New York, 277–304.

Doyle, P. S. and Riedel, W. R. (1979) Cretaceous to Neogene ichthyoliths in a giant piston core from the central North Pacific: *Micropaleontology* **25,** 337–364.

Duursma, E. K. and Hoede, C. (1967) Theoretical, experimental and field studies concerning molecular diffusion of radioisotopes in sediments and suspended solid particles of the sea. Part A. Theories and mathematical calculations: *Netherlands J. Sea Res.* **3,** 423–457.

Glasstone, S. (1946) *Textbook of Physical Chemistry:* 2nd ed., Van Nostrand Co., New York, 1047–1048.

Hayward, D. O. and Trapnell, B. M. W. (1964) *Chemisorption:* 2nd ed., Buttersworth, Washington, D.C., 159–225.

Heath, G. R., Epstein, G. B., Leinen, M., and Prince, R. A. (1977) Geochemical and sedimentological assessment of deep-sea sediments: in *Seabed Disposal Program Annual Report, January–December 1976,* Part 2, D. M. Talbert, ed., Sandia Laboratories, Albuquerque, New Mexico, Rept. **SAND78-1270,** 53–144.

Heath, G. R., Epstein, G. B., Leinen, M., and Prince, R. A. (1978) Geochemical and sedimentological assessment of deep-sea sediments: in *Seabed Disposal Program Annual Report, January–December 1977,* Part 2, D. M. Talbert, ed., Sandia Laboratories, Albuquerque, New Mexico, Rept. **SAND78-1359,** 33–188.

Heath, G. R., Laine, E. P., Heggie, D., Epstein, G. B., Leinen, M., and Prince, R. A. (1979) Geochemical and sedimentological assessment of deep-sea sediments: in *Seabed Disposal Program Annual Report, January–December 1978,* Part 2, D. M. Talbert, ed., Sandia Laboratories, Albuquerque. Rept. **SAND79-1618,** 121–236.

Heath, G. R. and Pisias, N. G. (1979) A method for the quantitative estimation of clay minerals in North Pacific deep-sea sediments: *Clays & Clay Minerals* **27,** 175–184.

Kolthoff, I. M. and Sandell, E. B. (1946) *Textbook of Quantitative Inorganic Analysis:* Macmillan, New York, 471–473.

Laudelout, H. R., Van Bladel, H. R., Bolt, G. H., and Page, A. L. (1968) Thermodynamics of heterovalent cation exchange reactions in a montmorillonite clay: *Trans. Faraday Soc.* **64,** 1477–1488.

Leinen, M. and Heath, G. R. (1981) Sedimentary indicators of atmospheric activity in the northern hemisphere during the Cenozoic: *Palaeogeog. Palaeoclimatol. Palaeoecol.* **36,** 1–21.

Li, Y.-H. and Gregory, S. (1974) Diffusion of ions in sea water and in deep-sea sediments: *Geochim. Cosmochim. Acta* **38,** 703–714.

Manheim, F. T. (1970) The diffusion of ions in unconsolidated sediments: *Earth Planet. Sci. Lett.* **9,** 307–309.

McBride, M. B. (1980) Interpretation of the variability of selectivity coefficients for exchange between ions of unequal charge on smectites: *Clays & Clay Minerals* **28,** 255–261.

Palmer, J. and Bauer, N. (1961) Sorption of amines by montmorillonite: *J. Phys. Chem.* **65,** 894–895.

Prince, R. A., Heath, G. R., and Kominz, M. (1980) Paleomagnetic studies of central North Pacific sediment cores: stratigraphy, sedimentation rates, and the origin of magnetic instability: *Geol. Soc. Amer. Bull.* **91,** 1789–1835.

Roache, P. J. (1972) *Computational Fluid Dynamics:* Hermosa Publishers, Albuquerque, New Mexico, 18–22.
Rodden, C. J. (1950) *Analytical Chemistry of the Manhattan Project:* McGraw-Hill, New York, 170–171, 183–184.

*(Received 17 July 1984; accepted 17 September 1985; Ms. 1389)*

APPENDIX I. Estimate of ΔH for the sorption of Th(IV) from 0.68 M NaCl solutions at 15°C onto Q1 sediment.

Regression of $\log(K_p)$ against $\log(C_s)$ and 1/T gives:

$$\log(K_p) = -0.8489 \log(C_s) - 836.53/T + 2.1953$$

(with a correlation coefficient of .9987). Rearranging:

$$\ln(M/C_s^{0.1511}) = 1926.19/T + 5.055.$$

Thus:

$$\frac{d \ln(K)}{d(1/T)} = -1926.19 = -\Delta H/R$$

so that ΔH = 3.83 kcal/mole.

APPENDIX II. Estimate of ΔH for the sorption of Th(IV) from 0.68 M NaCl solutions onto T2 sediment.

Regression of $\log(K_p)$ against $\log(C_s)$ and 1/T gives:

$$\log(K_p) = -0.7947 \log(C_s) - 363.19/T + 1.4986$$

(with a correlation coefficient of .9947). Rearranging:

$$\ln(M/C_s^{0.2053}) = -836.28/T + 3.4507.$$

Thus:

$$\frac{d \ln(K)}{d(1/T)} = -836.28 = -\Delta H/R$$

so that ΔH = 1.66 kcal/mole.

APPENDIX III. Estimate of the thermodynamic equilibrium constant (K) for the sorption of Eu(III) from NaCl solutions of various ionic strengths at 85°C onto T1 sediment.

Regression of $\ln(K_p)$ against $\ln(C_s)$ and ln(NaCl) gives:

$$\ln(K_p) = -0.8727 \ln(C_s) - 0.3978 \ln(NaCl) - 1.8628$$

(with a correlation coefficient of .9995). Rearranging:

$$\ln\left(\frac{M(NaCl)^{0.3978}}{C_s^{0.1273}}\right) = -1.8628.$$

Thus:

$$K = \frac{(M)(NaCl)^{0.3978}}{C_s^{0.1273}} = 0.1552.$$